High-Surface-Area Oxides Obtained by an Activated Carbon Route

Manfred Schwickardi, Thorsten Johann, Wolfgang Schmidt, and Ferdi Schüth*

Max-Planck-Institut für Kohlenforschung, Kaiser-Wilhelm-Platz 1, 45470 Mülheim, Germany

Received April 10, 2002. Revised Manuscript Received June 18, 2002

High-surface-area materials of various different compositions can be synthesized by a route involving impregnation of activated carbons with concentrated metal salt solutions and subsequent calcination to burn off the carbon material. This route allows the synthesis of a wide variety of different metal oxides, either as defined phases, if suitably chosen amounts of precursor salts are used, or as amorphous or partially crystalline multinary mixed-metal oxides. Typically, surface areas in the range between 50 and 200 m^2/g are accessible, and in addition to crystalline binary oxides, several high-surface-area spinels and perovskites can also be prepared.

1. Introduction

High-surface-area/small-particle-size materials are important in several application areas, such as catalysis, ceramics synthesis, adsorption, and others. There are numerous pathways leading to such materials from simple ones, such as precipitation, to quite intricate syntheses, such as reverse micelle synthesis, template routes, or controlled decomposition of defined precursor molecules. Several recent reviews and articles on the general pathways leading to high-surface-area materials and porous solids are available.[1−7] However, it is often especially difficult to produce high-surface-area ternary or multinary oxides, because their synthesis could require solid-state reactions from amorphous precursors involving high-temperature steps. At such high temperatures, sintering can be severe, resulting in the formation of large particles with correspondingly low surface areas.

There are several pathways to reduce these problems. One is to intimately mix the different metal centers on the atomic scale to minimize diffusion pathways for the formation of defined compounds, which normally results in a decrease of the temperatures necessary for the formation of the defined oxide phase. Sol−gel routes are very suitable, because the gentle conditions during the formation of the oxide/hydroxide networks allow the formation of atomically dispersed species if the hydrolysis rates of the precursors are matched. It is thus possible to create many different high-surface-area oxides[8] using this approach. Maier and co-workers[9] used sol−gel routes to produce amorphous mixed-metal oxides that have interesting textural properties and contain the constitutive elements mixed on the atomic level. Another route starting from atomically mixed compounds is the decomposition of defined precursor materials. For example, Schmidt and Weidenthaler[10] used differently ion-exchanged low-silica zeolites that were decomposed at high temperature to produce nanoparticle spinels in an amorphous silica matrix. After dissolution of the silica, high-surface-area spinels were obtained with surface areas up to about 200 m^2/g.

An alternative to atomically mixing the precursor elements is restricting the reaction space for the formation of the oxide/hydroxide, thus avoiding long diffusion distances. Reverse micelles, where micelles of an aqueous salt solution are dispersed in a continuous oil phase, have thus been used to carry out precipitation reactions in a constrained environment thereby avoiding the growth of large particles. Several multinary oxide materials have been produced by such routes, such as the barium hexaaluminate useful for the production of temperature-stable catalytic combustion catalysts.[11]

Although such methods are very valuable for the production of high-surface-area materials, they are typically either multistep procedures, such as the reverse micelle or zeolite precursor routes, or they involve costly reagents, such as alkoxides for the sol−gel synthesis route. Herein, we describe an alternative approach for the synthesis of high-surface-area materials that is quite versatile and can be used for the synthesis of a variety of different materials. It relies on the impregnation of activated carbon with highly concentrated metal salt solutions and subsequent calcina-

* To whom correspondence should be addressed. Phone: +49-(0)-208-306 2372. Fax: +49-(0)208-306 2995. E-mail: schueth@mpi-muelheim.mpg.de.

(1) Schüth, F. In *Handbook of Porous Solids*; Schüth, F., Sing, K., Weitkamp, J., Eds.; Wiley-VCH: Weinheim, Germany, 2002.
(2) Barton, T. J.; Bull, L. M.; Klemperer, W. G.; Loy, D. A.; McEnaney, B.; Misono, M.; Monson, P. A.; Pez, G.; Scherer, G. W.; Vartuli, J. C.; Yaghi, O. M. *Chem. Mater.* **1999**, *11*, 2633.
(3) Chuah, G. K. *Catal. Today* **1999**, *49*, 131.
(4) Walker, G. S.; Williams, A. K.; Bhattacharya, A. K. *J. Mater. Sci.* **1997**, *32*, 5583.
(5) Pierre, A. C.; Elaloui, E.; Pajonk, G. M. *Langmuir* **1998**, *14*, 66.
(6) Elaloui, E.; Pierre, A. C.; Pajonk, G. M. *J. Catal.* **1997**, *166*, 340.
(7) Mori, Y.; Okastu, Y.; Tsujimoto, Y. *J. Nanopart. Res.* **2001**, *3*, 219
(8) A good introduction is given in: Brinker, C. J.; Scherer, G. W. *Sol−Gel Science*; Academic Press: Boston, 1990.
(9) Maier, W. F.; Tilgner, I. C.; Wiedorn, M.; Ko, H. C. *Adv. Mater.* **1993**, *5*, 726.
(10) Schmidt, W.; Weidenthaler, C. *Chem. Mater.* **2001**, *13*, 607.
(11) Zarur, A. J.; Ying, J. Y. *Nature* **2000**, *403*, 65.

10.1021/cm0211857 CCC: $22.00
Published on Web 08/24/2002

Table 1. Selected Products Obtained via Impregnation of Activated Carbon with Concentrated Nitrate Precursor Solutions[a]

precursor	activated carbon	calcination	product (XRD)	surface area (BET) (m^2/g)	remarks
$Mg(NO_3)_2$	Darco KB-B	1 h, 500 °C	MgO	201	
$Mg(NO_3)_2$	−	1 h, 500 °C	MgO	9	
$Fe(NO_3)_3$	Fluka 05120	1 h, 450 °C	Fe_2O_3	123	
$Fe(NO_3)_3$	Darco KB-B	1 h, 450 °C	Fe_2O_3	113	
$Fe(NO_3)_3$	−	1 h, 450 °C	Fe_2O_3	36	
$Cr(NO_3)_3$	Fluka 05120	1.5 h, 450−500 °C	Cr_2O_3	156	with argon/air in a tube furnace
$Cr(NO_3)_3$	−	1 h, 500 °C	Cr_2O_3	10	
$Ti(OC_4H_9)_4$	Fluka 05120	1 h, 450 °C	TiO_2	200	
$Ti(OC_4H_9)_4$	−	1 h, 450 °C	TiO_2	43	
$Zn(NO_3)_2/Cr(NO_3)_3$	Fluka 05120	0.25 h, 800 °C	$ZnCr_2O_4$	72	
$Zn(NO_3)_2/Cr(NO_3)_3$	−	0.25 h, 800 °C	$ZnCr_2O_4$	8	
$Co(NO_3)_2/Cr(NO_3)_3$	Darco KB-B	1 h, 500 °C	$CoCr_2O_4$	126	
$Co(NO_3)_2/Cr(NO_3)_3$	Darco KB-B	0.75 h, 600 °C	$CoCr_2O_4$	111	
$Co(NO_3)_2/Cr(NO_3)_3$	−	0.75 h, 600 °C	$CoCr_2O_4$	27	multiphase
$Ni(NO_3)_2/Al(NO_3)_3$	Darco KB-B	5 h, 800 °C	$NiAl_2O_4$	165	
$Ni(NO_3)_2/Al(NO_3)_3$	Darco KB-B	0.25 h, 800 °C	$NiAl_2O_4$	220	
$Ni(NO_3)_2/Al(NO_3)_3$	−	0.25 h, 800 °C	$NiAl_2O_4$	106	multiphase
$La(NO_3)_3/Fe(NO_3)_3$	Fluka 05120	0.33 h, 700 °C	$LaFeO_3$	49	
$La(NO_3)_3/Fe(NO_3)_3$	−	0.33 h, 700 °C	$LaFeO_3$	14	multiphase

[a] Titanium tetrabutoxide was used neat.

tion to burn off the carbon. To the best of our knowledge, a similar approach has only been published once before, where ZrO_2 and a mixture of $Zr_2Nd_2O_7$ with ZrO_2 was obtained.[12] In addition, carbons have been used to synthesize zeolites in their pores,[13] and carbon fibers have been used to create an additional mesopore system in microporous materials such as zeolites.[14] A more complex procedure, using activated carbon as a template and involving impregnation in supercritical fluids, has also been described for the synthesis of nanoporous oxides.[15,16]

2. Experimental Section

Three different activated carbons were used for the experiments, including Darco KB-B (Aldrich, BET equivalent surface area of 1608 m^2/g), 05120 (Fluka, BET equivalent surface area of 1110 m^2/g), and 03866 (Fluka, BET equivalent surface area of 179 m^2/g). Many different metal salts were used for the impregnation of the carbons, including nitrates, alkoxides, chlorides, acetates, and acetylacetonates, mostly in the form of their most stable hydrates. The best results with respect to surface area were consistently found for the nitrates. In addition, the nitrates of most metals are highly soluble, which is advantageous in the process described here. Metal salts can also be dissolved in alcohols or other organic solvents, but the results reported here were all obtained from aqueous solutions or the neat alkoxides.

In a typical synthesis, the carbon powder was used as received. Activation at 100 °C in a vacuum prior to loading was also investigated, but results did not substantially differ for this method. Four milliliters of the appropriately concentrated metal salt solution, mostly as concentrated as possible, was added to 1.87 g of the carbon powder, and the mixture was kneaded using a spatula. This results in the formation of solid, crumbly particles. Alternatively, impregnation was performed with a slight excess of solution (1.7−1.8 g of carbon with 7 mL of solution) and 20 min of stirring. The slurry was then suction filtered and mechanically squeezed to remove the liquid on the surface of the carbon, which resulted in the formation of large oxide particles. The second impregnation pathway typically resulted in somewhat higher surface areas (about 10−20% higher).

These impregnated carbons were directly placed in a porcelain dish in a box oven and heated to the desired calcination temperature. In several cases, it was found advantageous to restrict the access of air during calcination by different methods, which are reported in the Results and Discussion section. After combustion of the carbon, the resulting oxide was stored for further characterization.

Samples were characterized by N_2 adsorption using a Micromeritics 2010 instrument at the temperature of liquid nitrogen. Prior to analysis, the samples were outgassed in a vacuum at 200 °C for 3−5 h. No microporosity was detected in any of the samples. BET surface areas were determined from the data points in the relative pressure range between 0.05 and 0.2.

XRD experiments were carried out in reflection geometry on a STOE STADI P Θ/Θ diffractometer using Cu Kα radiation. Scans were run with a step size of 0.04° 2Θ and a measurement time of 1−3 s per step, typically in the angle range between 10° and 80° 2Θ.

To follow the combustion process, TG/DTA experiments were performed using a Netzsch STA 449 C thermobalance. The standard heating rate in these experiments was 20 °C/min.

Selected samples were also analyzed by TEM (Hitachi H7500 or HF 2000). Samples were dispersed on holey carbon films on copper grids.

3. Results and Discussion

3.1. Binary Oxides. For all syntheses performed, it was consistently observed that the activated carbon route resulted in the formation of samples with surface areas substantially (4−20 times) higher than those of the control samples, which were performed by simply drying the corresponding salt solutions and then calcining them without carbon. Table 1 provides a survey of the materials synthesized via the carbon route, including the textural parameters and the crystallographic phase, together with the results of the corresponding blank experiments. As can be seen, a wide variety of oxide materials can be synthesized, the range of which is restricted only by the availability of suitable precursor salts. Nitrates were found to be best in all cases where a comparison was possible. For instance, MgO was also

(12) Ozawa, M.; Kimura, M. *J. Mater. Sci. Lett.* **1990**, *9*, 446.
(13) Madsen, C.; Jacobsen, C. J. H. *Chem. Commun.* **1999**, 673.
(14) Schmidt, I.; Boisen, A.; Gustavsson, E.; Stahl, K.; Pehrson, S.; Dahl, S.; Carlsson, A.; Jacobsen, C. J. H. *Chem. Mater.* **2001**, *13*, 4416.
(15) Fukushima, Y.; Wakayama, H. *J. Phys. Chem. B* **1999**, *103*, 3062.
(16) Wakayama, H.; Itahara, H.; Tatsuda, N.; Inagaki, S.; Fukushima, Y. *Chem. Mater.* **2001**, *13*, 2392

Table 2. Selected Products Obtained via Impregnation of Activated Carbon with Different Salt Solutions[a]

precursor	calcination[b]	heating rate (°C/min)	product (XRD)	surface area (BET) (m^2/g)
magnesium nitrate	1 h, 500 °C	2	MgO	171
magnesium acetate	1 h, 500 °C	2	MgO	48
magnesium chloride	1 h, 500 °C	2	MgO	30
magnesium sulfate	1 h, 500 °C	2	$MgSO_4$	14
magnesium stearate	1 h, 500 °C	2	?	39
iron(III) nitrate	1 h, 450 °C	4	Fe_2O_3	100
iron(III) chloride	1 h, 450 °C	4	Fe_2O_3	5

[a] The activated carbon Fluka 05120 used for all these experiments was dried at 100 °C and 0.1 mbar. [b] The samples were calcined in air in a box furnace at the given temperatures.

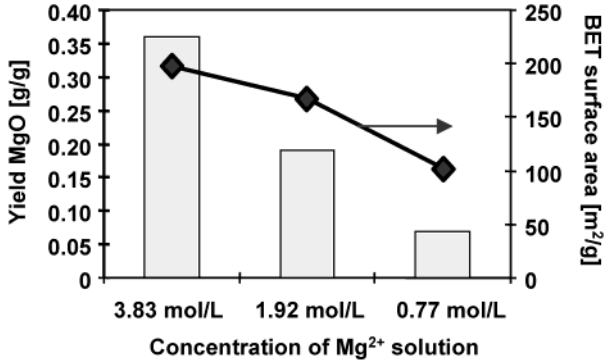

Figure 1. Yields and BET surface areas of MgO obtained by impregnating Darco KB carbon with $Mg(NO_3)_2$ solutions of different concentrations.

synthesized from the chloride and the acetate, Fe_2O_3 from iron(III) acetylacetonate, and titania from titanium tetrabutoxide. Table 2 provides examples of the results achieved with precursor salts other than nitrates for comparison. In other cases, different precursors were excluded without the syntheses actually being performed because of the low solubilities and the thus limited yields of oxide.

The type of carbon used has a substantial influence on the quality of the products. MgO was prepared starting from three different activated carbons. The sample prepared with the Darco KB-B carbon had a surface area of 190 m^2/g, whereas that prepared using Fluka 05120 resulted in the formation of MgO with a surface area of only 170 m^2/g, and that prepared using Fluka 03866 gave a product with a surface area of only 60 m^2/g. These textural data are typically reproducible to within 10%. Similar trends were also observed for other oxides. Whereas the first two types of carbons gave high-surface-area oxides, the Fluka 03866 carbon was not very suitable, because of either its different pore structure or its surface properties.

It is obviously desirable to load the carbons as high as possible to achieve a high yield of oxide product. High loadings with precursor solution also have another positive effect, which is shown here for the example of MgO but was also observed for other materials: The higher the concentration of the metal salt solution, the higher the specific surface area (Figure 1). Diluting the precursor solution by a factor of 5 results in a magnesium oxide with a surface area that is only about half that obtained from saturated precursor solution. The yield of the oxide obviously scales with the concentration

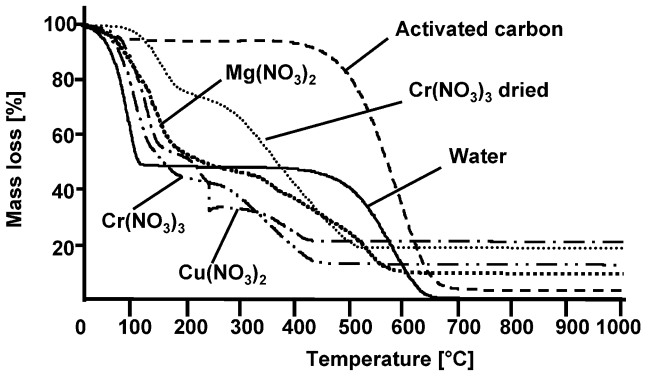

Figure 2. TG curves of different pure and impregnated carbon samples as labeled in the figure.

of the precursor solution, and essentially all of the metal precursor employed is recovered as oxidic material.

Although many different oxides can be synthesized following this route, some are more difficult to prepare with high surface area than others. One problem is the fact that the presence of the metal nitrate can catalyze the combustion of the activated carbon, which can then be quite vigorous. One should keep in mind that essentially an explosive is produced, containing a metal nitrate as an oxygen-containing compound and a high-surface-area carbon. TG/DTA studies were thus initiated to follow the combustion of the carbon. Figure 2 shows traces for several different samples. As can be seen, already $Mg(NO_3)_2$ catalyzes the combustion of the carbon, which probably occurs as a result of the presence of the nitrate rather than the Mg^{2+} present. With the transition metal nitrates, the effect is even more pronounced, pointing to a combined effect of the nitrate and the transition metal ion. The most pronounced catalytic effect is caused by the presence of copper, where an ignition takes place and the reaction is quite vigorous. This was also observed in preparative-scale experiments, where placing a $Cu(NO_3)_2$-impregnated carbon in a porcelain dish in the calcination oven led to such a vigorous reaction that the solid was ejected from the porcelain dish and could hardly be recovered. The powders collected afterward had surface areas below 10 m^2/g. This result is in line with the fact that copper is a component in soot oxidation catalysts; for instance, it is used in diesel exhaust streams.[17] On first sight, the fact that a material dried before combustion of the coal appears to show a slightly lower catalytic effect of the added salt is surprising. This fact will be addressed later in the discussion of the intermediate stages of coal combustion.

The observation of the very pronounced thermal effects up to an ignition phenomenon and the associated problems led to the investigation of gentler carbon-removal procedures. These studies were carried out with chromium nitrate impregnated carbon, because chromium nitrate leads to a vigorous combustion that can cause ignition but does not react as uncontrollably as the copper-containing material. Whereas the Cr_2O_3 prepared by the pathway described in the Experimental Section with a final temperature of 450 °C had a surface area of 70 m^2/g, already a simple measure such as

(17) Setzer, C.; Schütz, W.; Schüth, F. *Stud. Surf. Sci. Catal.* **1993**, *75*, 2629.

Table 3. Dependence of Surface Area and Residual Carbon Content of Fe_2O_3 on Calcination Time at 450 °C in a Fluidized Bed[a]

calcination time (h)	surface area (BET) (m^2/g)	carbon content (wt %)
0.5	108	1.67
1	108	0.89
2	106	0.15
6	97	0.08
18	83	0.05

[a] Sample obtained by impregnating Darco KB activated carbon with concentrated $Fe(NO_3)_3$ solution

placing a D2-glass frit on top of a quartz crucible before placing it in the oven to limit oxygen access to the powder resulted in the formation of a Cr_2O_3 with a surface area slightly above 100 m^2/g. To have an even more controlled combustion of the carbon, calcination was also carried out in a horizontal tube furnace in a quartz tube. Argon was first passed over the sample while the oven was being heated to 450 °C over 160 min, then the gas was switched to argon/air mixture (5:1) and heated to 500 °C for a time until the sample temperature no longer exceeded the oven temperature, which indicates full combustion of the carbon (approximately 1 h). The sample temperature was checked during this experiment by a thermocouple placed in the material. This procedure led to the formation of Cr_2O_3 with a surface area of 155 m^2/g. A comparable result was achieved by performing the carbon combustion in a fluidized bed in a vertical quartz tube. In this case, the sample was placed on a quartz frit at the bottom of the quartz tube and then fluidized by an argon/air (5:1) flow of 9 mL/s (for a tube 1.8 cm in diamter) while the oven was being heated to 450 °C. At the exit of the oven, the quartz tube widened to decrease linear flow velocity and prevent the loss of powder from the fluidized bed. The sample collected after this process had a surface area of 145 m^2/g. A thermocouple in the fluidized bed indicated that no overheating of the sample occurred during this process.

The kinetics of the fluidized-bed calcination was studied for the example of $Fe(NO_3)_3$-impregnated coal. For this purpose, the calcination was interrupted after defined periods of time, and the resulting material was analyzed by elemental analysis to determine the surface area and the amount of carbon still present. Table 3 reports the results. As one can see, even after relatively short times, the majority of the carbon was removed. The low levels of residual carbon are not expected to be a problem in most of the possible applications of such materials. Other systems were not studied as systematically in this respect, but the available data suggest that these results should be transferable to most other systems.

3.2. Ternary Oxides. If precursor nitrate solutions are mixed in the right proportion, defined solid-state phases of ternary oxides can be formed. Easily accessible by this approach are various different spinels. Aluminum-containing spinels had the highest specific surface areas; for instance, $NiAl_2O_4$ and $CoAl_2O_4$ after 15 min of calcination at 800 °C had surface areas of more than 200 m^2/g. Also, several chromium spinels, such as $ZnCr_2O_4$ and $CoCr_2O_4$, were prepared that had surface areas of around 80 m^2/g. When comparing surface areas of the aluminum and the chromium spinels, one should keep in mind that the chromium spinels have higher densities and thus, even for identical particle sizes, will give lower specific surface areas. The XRD patterns of all of these materials are characteristic of the pure spinel phase (an example is presented in Figure 3). The particle sizes calculated from the line broadening of the XRD reflections using the Scherrer equation agree reasonably well with those calculated from the BET surface area assuming spherical particles [3 nm (XRD) versus 8 nm (BET) for $NiAl_2O_4$, 7 nm (XRD) versus 11 nm (BET) for $CoCr_2O_4$]. Also, the particle sizes obtained by TEM correspond to those given above, as shown in Figure 4 for $NiAl_2O_4$ with an approximate particle size of 6 nm.

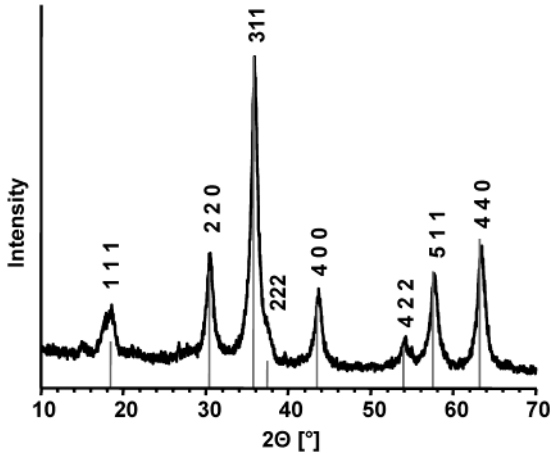

Figure 3. XRD pattern of $CoCr_2O_4$ synthesized by impregnating Darco KB carbon with appropriate amounts of concentrated $Co(NO_3)_2$ and $Cr(NO_3)_3$ solutions (lines indicate spinel reflections according to PDF-2 entry 22-1084).

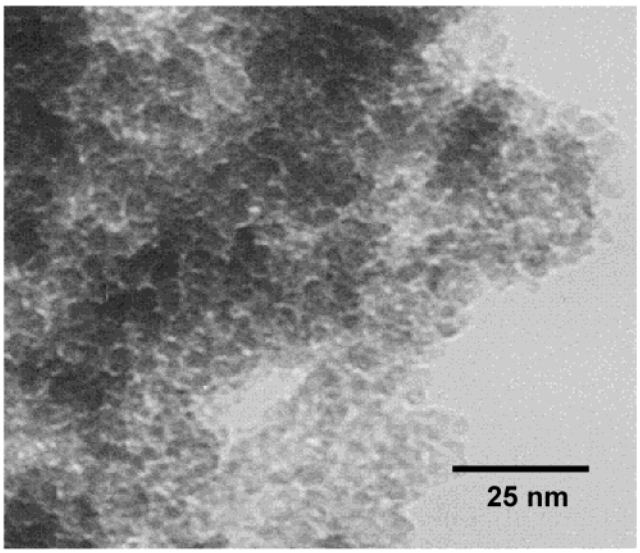

Figure 4. TEM image of a typical $NiAl_2O_4$ spinel obtained by impregnating Darco KB carbon with appropriate amounts of concentrated $Ni(NO_3)_2$ and $Al(NO_3)_3$ solutions.

A particular challenge is the production of perovskites with high surface areas, because such materials are interesting as, for instance, catalysts in $DeNO_x$ reactions[18] or as sensor materials.[19] The production of

(18) Labhsetwar, N. K.; Watanabe, A.; Biniwale, R. B.; Kumar, R.; Mitsuhashi, T. *Appl. Catal. B: Environ.* **2001**, *33*, 165 and references therein.

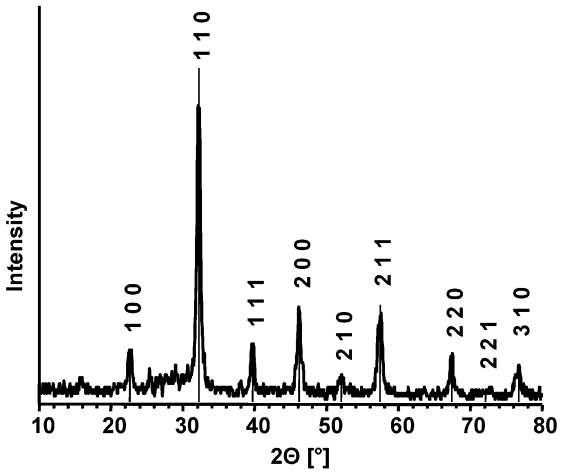

Figure 5. XRD pattern of $LaFeO_3$ perovskite obtained by impregnating Fluka 05120 carbon with appropriate amounts of concentrated $La(NO_3)_3$ and $Fe(NO_3)_3$ solutions (lines indicate perovskite reflections according to PDF-2 entry 75-541).

perovskites following the pathway introduced above is not straightforward, because for many of the perovskite-forming elements, no highly soluble precursor salts are available. However, it was nevertheless possible to synthesize the perovskite $LaFeO_3$ with a specific surface area of 50 m^2/g (Figure 5). A reference experiment in which the metal nitrate solutions were mixed, dried, and calcined did lead to a low-surface-area material that did not even have the perovskite structure. The production of a $BaZrO_3$ perovskite from $Ba(NO_3)_2$, $ZrO(NO_3)_2$, and HNO_3 to maintain sufficient solubility of the precursor salts was also attempted. In this experiment, the perovskite was again formed, but some unidentified impurity phase was also present after calcination at 800 °C. The surface area of this material was 21 m^2/g, whereas a reference sample had a surface area below 1 m^2/g. Calcination at 1000 °C gave a pure perovskite; the surface area, however, was reduced to about 8 m^2/g.

It is expected, though, that, by judicious choice of precursor salts, a much wider range of perovskites or other ternary oxide structures will be accessible and that it will be possible to further increase surface areas.

3.3. Amorphous or Partly Amorphous Multinary Oxides. The synthesis pathway can be used not only to produce oxides with a defined solid-state structure, but also to synthesize multinary oxides that are amorphous or partly amorphous with crystalline components. Essentially any mixture of nitrate precursor solutions can be combined to result in the formation of mixed oxides or oxide mixtures. Depending on the nature of the precursors and their relative ratios, amorphous, partly amorphous, or crystalline materials can be formed. The synthesis process lends itself easily to parallelization, which we have pursued to integrate this synthesis method into our program on high-throughput experimentation in heterogeneous catalysis. To this end, different precursor components out of a total of 10 in random relative amounts are selected by a computer program, and the relative amounts are recalculated to give solution volumes to be impregnated. These data are stored on a disk that is transferred to a synthesis robot,

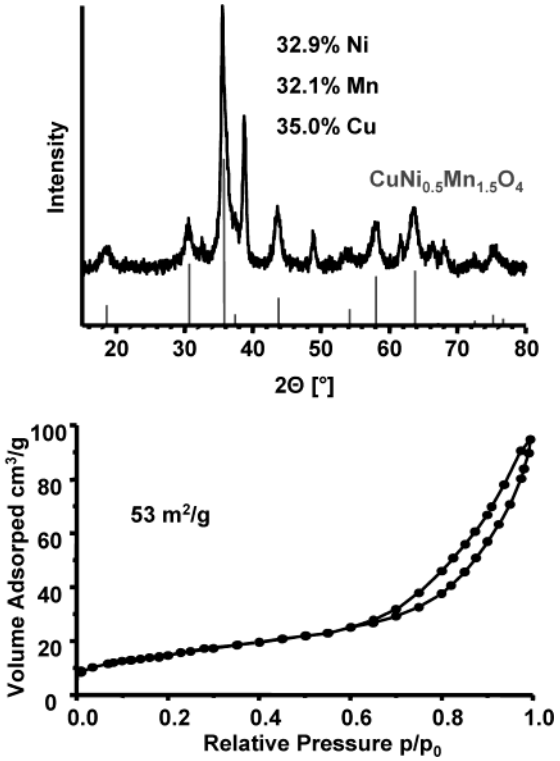

Figure 6. XRD pattern (top) and nitrogen sorption isotherm (bottom) of a typical product from the synthesis of multinary oxides via the activated carbon route. The composition adjusted in the impregnation solution corresponds to 32.9% Ni, 32.1% Mn, and 35% Cu. The lines correspond to reflections of the spinel $CuNi_{0.5}Mn_{1.5}O_4$ (PDF-2 entry 80-2185), which suggests that this or a related phase is predominantly formed.

which then simultaneously produces 77 different materials. These materials are subsequently calcined simultaneously with the same heating program. We have so far synthesized several hundred different compositions and characterized many of them by sorption, TEM, EDX, and XRD. In general, the more common mixed-metal oxides, such as spinels, form in a matrix of amorphous product. Typical surface areas are in the range of 70 m^2/g, with interparticle pores in the mesopore range. Figure 6 shows a representative diffraction pattern and sorption isotherm for one such material. A clear structural assignment of the diffraction pattern is not possible. It corresponds to the expected pattern of a spinel, but the *d* spacing does not correspond exactly to that of any known spinel phase containing the elements present in the sample. It is probably a spinel with several of the elements at both tetrahedral and octahedral sites.

We think that this synthesis pathway will prove to be very useful, especially if carried out in the high-throughput mode. In addition to the simple generation of a large number of different high-surface-area oxides, this approach allows the rapid sampling of phase diagrams or synthesis field diagrams for multinary oxide systems, if coupled to a high-throughput X-ray analysis that has already been used for other purposes.[20]

3.4. Intermediate Stages during Oxide Formation. For better control of the formation process and the properties of the resulting oxides, the detection of

(19) Ramirez-Salgado, J.; Fabry, P. *Sens. Actuators B: Chem.* **2002**, *82*, 34.

(20) Klein, J.; Lehmann, C. W.; Schmidt, H. W.; Maier, W. F. *Angew. Chem., Int. Ed. Engl.* **1998**, *37*, 3369.

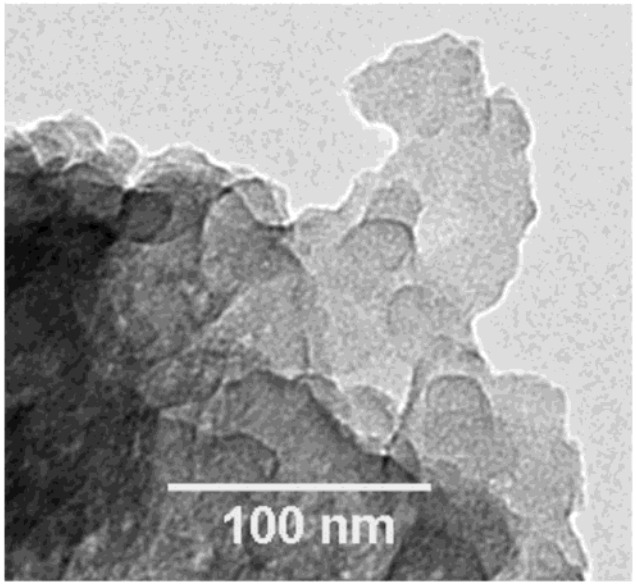

Figure 7. TEM image of a Darco KB activated carbon impregnated with $Mg(NO_3)_2$.

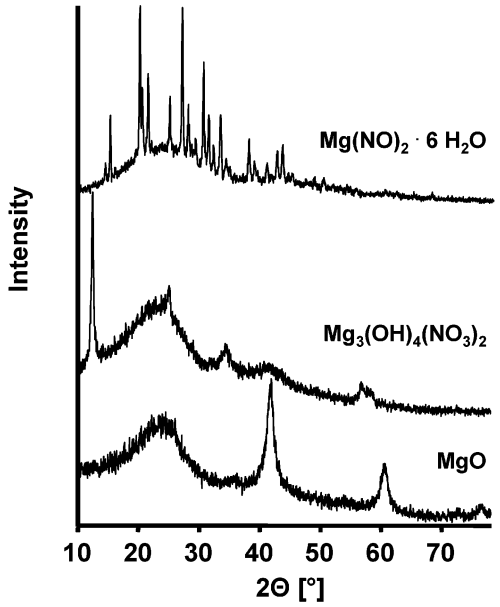

Figure 8. XRD patterns of activated carbon impregnated with $Mg(NO_3)_2$ after drying at room temperature with the reflections of $Mg(NO)_2 \cdot 6H_2O$ (top), after drying at 170 °C with some reflections corresponding to basic magnesium nitrate $Mg_3(OH)_4(NO_3)_2$ (middle), and after calcination at 400 °C with two reflections corresponding to MgO. The intensity scales for the different patterns are not identical, but the patterns were recorded under the same conditions. The signal-to-noise ratio thus provides information on the relative intensities of the different reflections.

intermediate stages during the transformation from the carbon-confined nitrates to the oxide material was attempted. For this purpose, the precursor materials MgO, $NiAl_2O_4$, and $LaFeO_3$ were calcined either in quartz crucibles covered with D2 frits in the box furnace or in the fluidized bed at different temperatures. The resulting materials were analyzed by TEM and XRD and, in selected cases, by nitrogen adsorption.

No features indicative of crystalline phases could be detected in the impregnated carbon by TEM. Figure 7 shows a dried sample of an activated carbon that had been impregnated with $Mg(NO_3)_2$. This image is typical for all samples analyzed. Only in the case of heavier elements were stronger contrasts observed, but again, no crystalline phases were detected. In most cases, intermediate crystalline phases were also not detected by XRD. Only for magnesium nitrate-impregnated carbon was some $Mg(NO_3)_2 \cdot 6H_2O$ detected if the samples were dried at room temperature for 21 h in air. If a slight excess of impregnation solution was used, basic magnesium nitrate hydrate, $Mg_3(OH)_4(NO_3)_2$, was occasionally found (Figure 8). However, when the samples were dried at 80 °C for the same time, no nitrate reflections were detected, only the background diffraction pattern of the activated carbon. Probably drying at room temperature is sufficiently slow to allow some transport of the magnesium nitrate out of the carbon pore system and subsequent formation of nitrate particles large enough to be detected by XRD. A related effect is observed in the preparation of supported catalysts, where the active component is primarily located near the external surface of catalyst particles after slow drying of the impregnated particles. This magnesium nitrate outside the carbon pore system is probably also the reason for the lower catalytic effect of magnesium nitrate upon combustion for the dried sample in comparison with the fresh sample directly investigated by TG (Figure 2).

For the MgO/activated carbon system, first indications of MgO formation are observed after heating to only 170 °C (Figure 8). The diffraction pattern then does not change substantially at higher temperatures. Only the background that can be attributed to the activated carbon is reduced, because the carbon is removed during the calcination process.

For the spinel and the perovskite, no intermediate crystalline phases were detected for either the nitrates or the binary oxides before the reflections of the spinel or the perovskite appeared. Drying a mixture of the precursor nitrate solutions without the carbon resulted in a material that showed a diffraction pattern corresponding to a mixture of the metal nitrates, as expected.

These data shed some light on the effect the carbon has on the formation of the high-surface-area materials. The narrow pore system of the activated carbon effectively prevents the formation of large nitrate precursor particles during drying and heating. The average pore size of the carbons is around 4−6 nm (with a rather broad distribution though), which would correspond to typical domain sizes of solution in the pores. If this solution evaporates, small nitrate particles will result that will have sizes on the order of nanometers, which means that they would not be detectable by X-ray diffraction. This confinement effect is most probably also the origin of the high surface areas. If the oxide particles are formed before the carbon is combusted, either as amorphous precursors, as in the case of the spinels or the perovskites, or in crystalline form, as for the binary oxides, they will not grow further and will remain in the state of nanoparticles with correspondingly high surface areas. If the transformation of the nitrates to oxides occurs simultaneously with the combustion of the carbon or even after the combustion, the confinement effect cannot manifest itself, and the resulting oxide

powder will have relatively large particles and a low surface area. This is probably the case for the $Cu(NO_3)_2$/activated carbon system, where the removal of the catalyzed carbon proceeds at such low temperature that, afterward, coalescence of the copper nitrate/oxide particles occurs. Also, the improved textural parameters of the chromium oxides synthesized with the D2 frit or initially with argon to delay the carbon combustion are most probably due to the existence of the pore system of the carbon until a sufficiently high temperature is reached so that the oxide is already formed.

One should mention here that, for some of the more easily reduced metal ions, intermediate reactions might take place during carbon removal. In the final materials, no such states could be detected, nor did they appear as intermediate low-valence crystalline phases. Work using XPS on intermediates of the transformation on selected samples is in progress to address this question.

4. Conclusion

We have described a widely applicable pathway for the formation of high-surface-area binary, ternary, and multinary oxides that can either be amorphous or have a defined crystalline structure, such as the spinel or the perovskite structure. The high surface area is probably induced by the confinement brought about by the activated carbon pore system, which prevents growth of the particles before the oxides with limited mobility of the constituents have been formed.

We expect this pathway to be useful in the facile preparation of various oxide materials that can then be used in different applications or, especially in the parallelized mode, as a simple tool for the evaluation of phase diagrams and synthesis field diagrams of multinary oxides. Compared to other complex routes to high-surface-area oxides, this pathway seems easily scalable, using either the fluidized-bed process described or industrial ovens such as rotary kilns. The costs of bulk amounts of activated carbons are reasonable, so that the route is also economically viable. One major problem is the release of nitrogen oxides during calcination. However, technology is available that can deal with such emissions, especially if they are generated in a localized region. Moreover, many other synthesis pathways also rely on nitrate precursors with identical associated problems. Several interesting catalytic reactions are presently under scrutiny that employ oxides synthesized via the activated carbon route, and it is expected that improvements over existing technology are indeed possible.

Acknowledgment. We thank O. Busch for support in the parallelization of the synthesis and A. Dreier and B. Spliethoff for the TEM analysis. This work is dedicated to Prof. Dr. J. Weitkamp on the occasion of his 60th birthday.

CM0211857